Optics Letters

Photonic crystal-based compact hybrid WDM/MDM (De)multiplexer for SOI platforms

Omnia M. Nawwar,[1,2,3,*] Hossam M. H. Shalaby,[1,3] and Ramesh K. Pokharel[2]

[1]Department of Electronics and Communications Engineering, Egypt-Japan University of Science and Technology (E-JUST), Alexandria 21934, Egypt
[2]Graduate School of Information Science and Electrical Engineering, Kyushu University, Fukuoka 819-0395, Japan
[3]Electrical Engineering Department, Faculty of Engineering, Alexandria University, Alexandria 21544, Egypt
*Corresponding author: omnia.nawwar@ejust.edu.eg

Received 21 June 2018; revised 25 July 2018; accepted 26 July 2018; posted 27 July 2018 (Doc. ID 335811); published 24 August 2018

A compact hybrid wavelength- (WDM) and mode-division (de)multiplexer (MDM) is proposed, and its performance is evaluated. The design of the device is based on 2D photonic crystals with a square lattice and Si rods. The device can multiplex two eigenmodes, TM_0 and TM_1, and two wavelengths, 1550 and 1300 nm. Two identical multimode interference couplers and an asymmetric directional coupler are used in implementing both the wavelength- and mode-division multiplexing functions, respectively. To avoid back-reflections, tapers are used at waveguide junctions. The structure is compact with dimensions of 29 μm × 12 μm, which is suitable for on-chip integration. Simulation results reveal that the insertion losses and crosstalks are less than −1.0927 and −11.9024 dB, respectively, for all four channels.

OCIS codes: (130.0130) Integrated optics; (230.5298) Photonic crystals; (130.5296) Photonic crystal waveguides; (230.3120) Integrated optics devices.

https://doi.org/10.1364/OL.43.004176

Hybrid multiplexing techniques have been proposed as an efficient way to increase the capacity of optical communications systems [1,2]. In optical networks, wavelength-division multiplexing (WDM) has been used for a long time to multiplex different channels into the same medium. In such systems, multiple laser sources with different wavelengths have to be used which increase system complexity and cost [3,4]. It has been realized using different schemes such as directional couplers (DCs), ring resonators (RRs), and multimode interference (MMI) couplers [5–10]. To keep up with the increasing demand of system capacity and data rates, mode-division multiplexing (MDM) has emerged which obviates the need for multiple laser sources by carrying the data on different modes instead of wavelengths [2,11,12]. It has been realized for on-chip interconnect using a lot of approaches. DCs, Bragg gratings, RRs, MMIs, and asymmetric Y-junction techniques have been proposed in the literature [13–19].

Photonic crystals (PhCs) have been proposed to realize photonic integrated circuits (PICs) due to their good performance and compactness [20–22]. The photonic bandgap created from the periodically modulated refractive index has been used to control and manipulate light in different ways [23,24]. A variety of devices have been implemented using PhCs with promising performance and compactness compared to conventional counterparts [20–22,25–27]. Hybrid WDM/MDM systems have been investigated in Refs. [28–33]. In Ref. [30], a WDM/MDM system has been proposed for an silicon-on-insulator (SOI) platform. It uses strip waveguides to implement MMI and DCs for the multiplexing process. Although its performance is good, the footprint is large. The same size problem has appeared in Ref. [31], which has been realized using cascaded RRs and DCs.

In this Letter, we propose a very compact PhC device for implementing a hybrid WDM/MDM system. The size is highly reduced (29 μm × 12 μm) compared to similar devices using conventional waveguides. The proposed device has good performance and is expandable by adding more MMI units and using wider bus waveguides. The performance for each section is evaluated using FDTD simulations to give more insight into the device performance. Our proposed structure is based on square lattice silicon (Si) rods and air background. Similar square lattice structures have been proposed in the literature for Si/SiO_2 material systems. They have also been fabricated and tested [34,35]. Conventional SOI fabrication techniques can be used in the fabrication process. The parameters of the guided modes are extracted from the band structure. The proposed structure is compact with good insertion losses (ILs) and crosstalks, which makes it suitable for PIC applications.

The rest of this Letter is organized as follows. The band structure of the used lattice is introduced, and the operation principle is discussed. Then, mode and wavelength (de)multiplexer parameters are extracted. The whole performance of proposed architecture is evaluated. Finally, the conclusion is stated.

The proposed WDM/MDM structure is shown in Fig. 1. Two identical MMIs and an asymmetric DC are used. In this structure, two wavelengths and two eigenmodes are multiplexed. Four data channels are excited at the four input ports

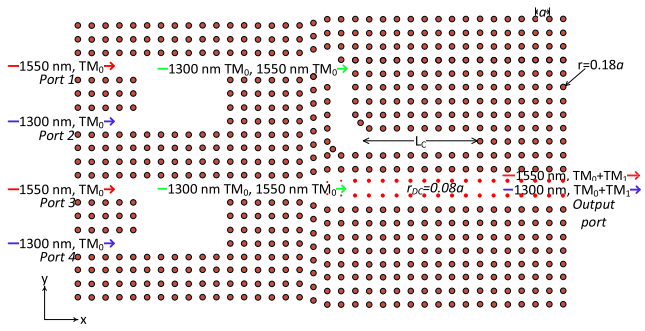

Fig. 1. Detailed structure for the proposed WDM/MDM (de)multiplexer.

of two MMIs, which multiplex a couple of wavelengths together into the outputs of the MMIs. Next, one asymmetric DC is used to raise the mode order of two data channels from one MMI to the first-order mode in the bus waveguide. In this case, the MDM should have good performance for both wavelengths simultaneously. The proposed structure has the advantage of being scalable by adding more MMI units and making the bus waveguide wider.

A square lattice with lattice constant a is used with Si rods of radius $r = 0.18a$ and air background. For this lattice, an optical bandgap is opened from 0.3076 to 0.4443 in a/λ units for TM-polarized modes, where λ is the free space wavelength. (The E component is normal to the PhC plane.) By introducing a defect to the perfect crystal, light can be controlled and manipulated in different ways. The band structure of a one-row defect waveguide, used as input and output arms of MMI, is shown in Fig. 2(a). A five-row defect waveguide, used as an MMI region, would support five modes, as shown in Fig. 2(b). Two normalized frequencies, $0.3405(a/\lambda)$ and $0.4081(a/\lambda)$, are chosen within the bandgap. At a period of 528 nm, these frequencies correspond to wavelengths of 1550 and 1300 nm, respectively.

A wavelength (de)multiplexer is implemented using the MMI unit. The MMI operation is based on a self-imaging principle to produce multiple images of an input light signal at different positions of the MMI region. As the MMI region is a five-row defect multimode waveguide, there are five guided modes in this region. The band structure of the MMI region with the allowed modes can be seen in Fig. 2(b). In the literature, PhC MMI has been proposed to operate as WDM with single-mode input and output arms [4,7]. In our case, we use two identical MMIs separated by a distance $3a$ to perform WDM multiplexing. Both MMIs are swept at the same time to take into account the mutual effect between both of them. At an MMI length of $26a$, the ILs are 0 dB, −0.0864, −0.0178, and −0.1265 dB for the four ports. Figure 3 shows the E_z component for all channels in the two MMIs.

The two output waveguides from both MMIs are then injected into an asymmetric DC to implement the MDM function. The DC is formed by placing two waveguides in parallel. The access waveguide is a single-mode waveguide formed by removing one row of the crystal, while the bus waveguide is formed by readjusting the rod radius of two rows, r_{DC}. The two waveguides have two row separations between them. The propagation constants of the fundamental mode in the

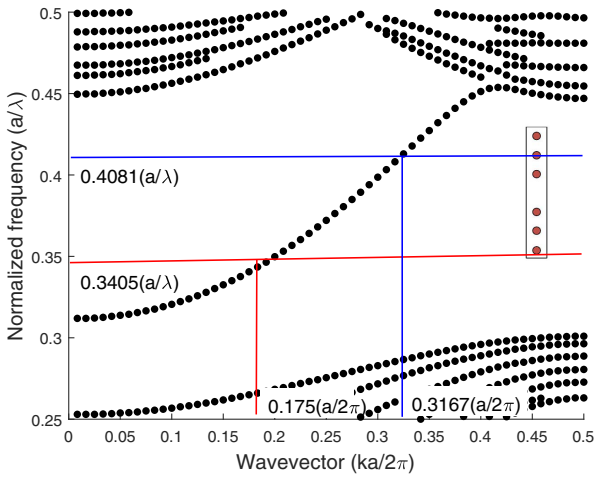

Fig. 2. (a) Band structure of a one-row defect waveguide. Only one mode is supported in the bandgap. (b) Band structure of a five-row defect waveguide of the MMI region.

access waveguide at 1550 and 1300 nm are $0.175(a/2\pi)$ and $0.3167(a/2\pi)$, respectively, as shown in 2(a). The relation between the rod radius in the bus waveguide and the propagation constant of the first-order mode for both wavelengths is given in Fig. 4. The DC adjusted rod radius r_{DC} is chosen as $0.08a$, which results in a phase mismatch at both wavelengths. This value is negligible, as can be calculated from Fig. 4.

The upper MMI output goes through a bend to the access waveguide. The bend used has two rods added at the corners of the bend to achieve a smooth transition to the access waveguide. These rods are shifted by $\pm a/2$ in x and y from its original location. The E_z component for both wavelengths is shown in Fig. 5. As only TM_1 satisfies the phase-matching condition with the fundamental mode in an access waveguide, coupling to it will occur. At a coupling length of $L_c = 15a$, the IL of the bend and the DC at 1550 and 1300 nm are −0.9620 and −1.0353 dB, respectively. If the coupling length is chosen incorrectly, the signal will not be able to couple to the output port which causes back-reflection in the device.

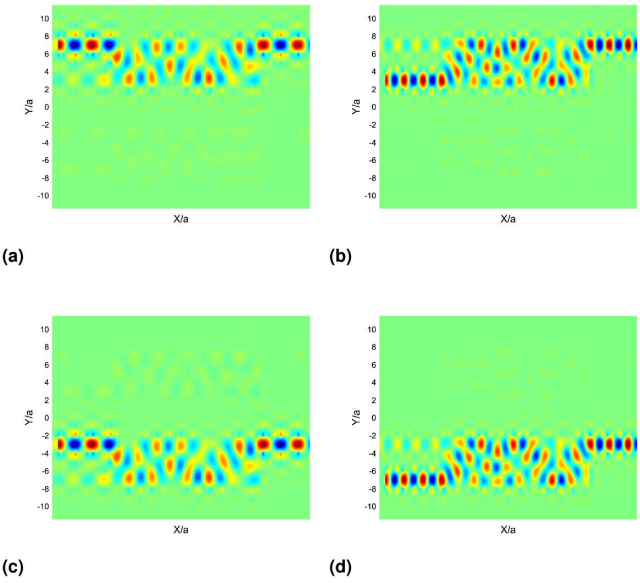

Fig. 3. E_z component propagation in both MMIs for (a), (c) ports 1, 3 at 1550 nm and (b), (d) ports 2, 4 at 1300 nm.

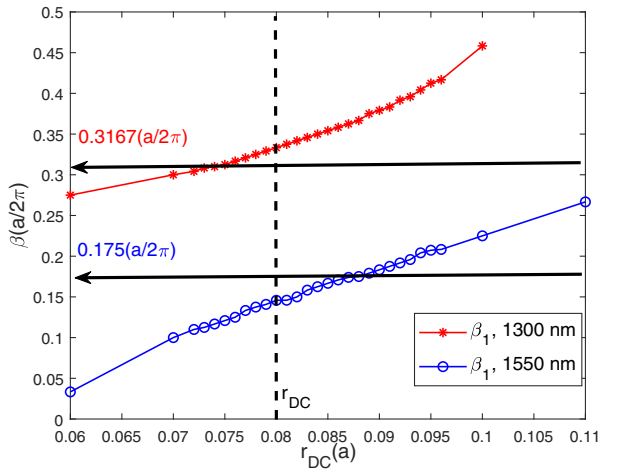

Fig. 4. Relation between the adjusted rod radius in a bus waveguide and propagation constant of the first-order mode at two wavelengths.

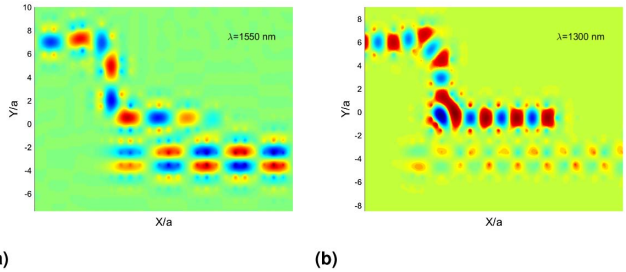

Fig. 5. Mode conversion function with a coupling length 15a for (a) 1550 and (b) 1300 nm.

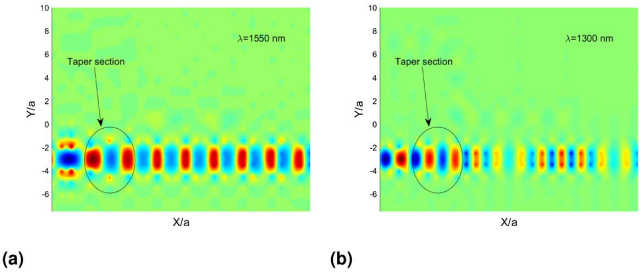

Fig. 6. E_z component through a taper with length 3a for (a) 1550 and (b) 1300 nm.

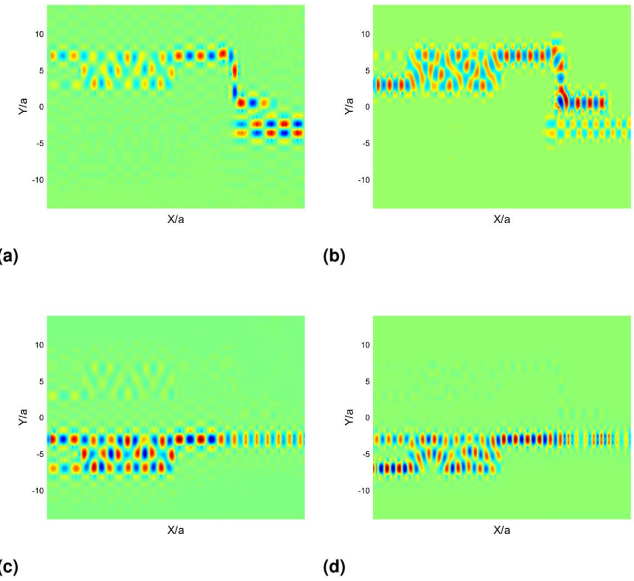

Fig. 7. E_z components in the whole structure for four input ports. (a), (c) Conversion of two 1550 nm channels to first-order and fundamental modes in a bus waveguide, respectively; (b), (d) conversion of two 1300 nm channels to first-order and fundamental modes, respectively.

For signals from ports 3 and 4, a taper should be designed at a waveguide junction to prevent back-reflection and ensure smooth transition to the desired mode. The taper has a length of 3a, and its width increases gradually from a to 2a. Figure 6 shows the transition through the taper to the output port. The taper has gradual embedded rod radii of $r_{DC}/4$ and $r_{DC}/2$. The ILs at 1300 nm is lower than that at 1550 nm. The ILs are −0.2156 and −0.0640 dB at 1550 and 1300 nm, respectively.

As indicated in Fig. 1, the light at ports 1 and 3 has a wavelength of 1550 nm, while that at ports 2 and 4 has a wavelength of 1300 nm. The overall performance of this architecture is shown in Fig. 7. The transmission is found to be −1.0927, −0.9745, −0.3580, and −1.0395 dB for the four channels. The overall area of this structure is 55a × 23a.

As all components have symmetric properties, the device can also operate as a demultiplexer. That is, we can excite two eigenmodes at 1550 and 1300 nm and get them from different ports. When exciting the fundamental and first-order mode at 1550 nm from the output port, we get IL of −0.2466 and

Table 1. Crosstalks on All Ports for the Proposed Structure When Working as a DEMUX

	Port 1	Port 2	Port 3	Port 4
TM_0, 1550 nm	−26.6959 dB	−24.1454 dB		−14.0594 dB
TM_1, 1550 nm		−11.9024 dB	−36.2709 dB	−32.6922 dB
TM_0, 1300 nm	−36.5639 dB	−21.8582 dB	−11.9723 dB	
TM_1, 1300 nm	−11.5021 dB		−30.0568 dB	−14.7444 dB

−0.3401 dB at ports 3 and 1, respectively. In the case of the fundamental mode at 1300 nm, the IL at port 4 is −0.3203 dB, while the IL for the first-order mode at the same wavelength is −0.4832 dB at port 2. The corresponding crosstalks are indicated in Table 1. The worst crosstalk for all channels is −11.5021 dB.

A hybrid WDM/MDM (de)multiplexer, based on PhCs, has been proposed. Two wavelengths, 1550 and 1300 nm, and two eigenmodes, fundamental and first-order modes, have been (de)multiplexed using the proposed device. The structure has the advantage of scalability to add more wavelengths by simply adding more WDM units, and more modes by using a wider bus waveguide. The performance of the device has been evaluated for both multiplexer and demultiplexer operations. Our results reveal that the ILs for all channels are less than −1.0927 dB.

Funding. Egyptian Ministry of Higher Education (MoHE), Egypt; E-JUST Center of Kyushu University, Japan.

REFERENCES

1. T. Ohara, H. Takara, I. Shake, K. Mori, S. Kawanishi, S. Mino, T. Yamada, M. Ishii, T. Kitoh, T. Kitagawa, K. R. Parameswaran, and M. M. Fejer, IEEE Photon. Technol. Lett. **15**, 302 (2003).
2. D. Dai, C. Li, S. Wang, H. Wu, Y. Shi, Z. Wu, S. Gao, T. Dai, H. Yu, and H. Tsang, Laser Photon. Rev. **12**, 1700109 (2018).
3. C. A. Brackett, IEEE J. Sel. Areas Commun. **8**, 948 (1990).
4. S. Zhang, W. Ji, R. Yin, X. Li, Z. Gong, and L. Lv, IEEE Photon. Technol. Lett. **30**, 107 (2018).
5. M. Koshiba, J. Lightwave Technol. **19**, 1970 (2001).
6. G. Manzacca, D. Paciotti, A. Marchese, M. S. Moreolo, and G. Cincotti, Photon. Nanostruct. **5**, 164 (2007).
7. H. J. Kim, I. Park, B. H. O, S. Park, E. Lee, and S. G. Lee, Opt. Express **12**, 5625 (2004).
8. L. W. Chung and S. L. Lee, Opt. Express **14**, 4923 (2006).
9. B. Wang, X. Chen, and D. Yang, in *Conference on Lasers and Electro-Optics Pacific Rim (CLEO-PR)*, Singapore, Singapore, 2017.
10. S. M. Mirjalili and S. Z. Mirjalili, Neural Comput. Appl. **28**, 1463 (2017).
11. S. Berdagué and P. Facq, Appl. Opt. **21**, 1950 (1982).
12. N. Bozinovic, Y. Yue, Y. Ren, M. Tur, P. Kristensen, H. Huang, A. Willner, and S. Ramachandran, Science **340**, 1545 (2013).
13. Y. Ding, J. Xu, R. Da, B. Huang, H. Ou, and C. Peucheret, Opt. Express **21**, 10376 (2013).
14. J. Driscoll, R. Grote, B. Souhan, J. Dadap, M. Lu, and R. Osgood, Opt. Lett. **38**, 1854 (2013).
15. J. Wang, S. He, and D. Dai, Laser Photon. Rev. **8**, L18 (2014).
16. H. M. H. Shalaby, J. Lightwave Technol. **34**, 3633 (2016).
17. O. Nawwar, H. Shalaby, and R. Pokharel, Appl. Opt. **57**, 42 (2018).
18. L. Chen, Y. Wei, X. Zang, Y. Zhu, and S. Zhuang, Sci. Rep. **6**, 22027 (2016).
19. L. Chen, N. Xu, L. Singh, T. Cui, R. Singh, Y. Zhu, and W. Zhang, Adv. Opt. Mater. **5**, 1600960 (2017).
20. T. Liu, A. R. Zakharian, M. Fallahi, J. V. Moloney, and M. Mansuripur, J. Lightwave Technol. **22**, 2842 (2004).
21. H. S. Kim, T. K. Lee, G. Y. Oh, and Y. W. Choi, in *15th OptoElectronics and Communications Conference*, Sapporo, Japan, 2010.
22. D. Gailevicius, V. Koliadenko, and V. Purlys, in *19th International Conference on Transparent Optical Networks (ICTON)*, Girona, Spain, 2017.
23. A. Young, A. Thijssen, D. Beggs, P. Androvitsaneas, L. Kuipers, J. Rarity, S. Hughes, and R. Oulton, Phys. Rev. Lett. **115**, 153901 (2015).
24. S. Yan, X. Zhu, L. Frandsen, S. Xiao, N. Mortensen, J. Dong, and Y. Ding, Nat. Commun. **8**, 14411 (2017).
25. L. O'Faolain, D. M. Beggs, T. P. White, T. Kampfrath, K. Kuipers, and T. F. Krauss, IEEE Photon. J. **2**, 404 (2010).
26. K. Inoue and K. Ohtaka, *Photonic Crystals: Physics, Fabrication and Applications* (Springer, 2013), Vol. **94**.
27. V. Liu, D. A. B. Miller, and S. Fan, Opt. Express **20**, 28388 (2012).
28. J. B. Driscoll, C. P. Chen, R. R. Grote, B. Souhan, J. I. Dadap, A. Stein, M. Lu, K. Bergman, and R. M. Osgood, Opt. Express **22**, 18543 (2014).
29. L. W. Luo, N. Ophir, C. P. Chen, L. H. Gabrielli, C. B. Poitras, K. Bergmen, and M. Lipson, Nat. Commun. **5**, 3069 (2014).
30. T. Mulugeta and M. Rasras, Opt. Express **23**, 943 (2015).
31. Y. D. Yang, Y. Li, Y. Z. Huang, and A. W. Poon, Opt. Express **22**, 22172 (2014).
32. Y. Fazea and A. Amphawan, J. Opt. Commun. **36**, 327 (2015).
33. Y. Fazea and A. Amphawan, J. Opt. Commun. **39**, 175 (2016).
34. M. Loncar, T. Doll, J. Vuckovic, and A. Scherer, J. Lightwave Technol. **18**, 1402 (2000).
35. J. Lee, B. Zhen, S. Chua, W. Qiu, J. D. Joannopoulos, M. Soljacic, and O. Shapira, Phys. Rev. Lett. **109**, 067401 (2012).